Walking elicits global brain activity in *Drosophila*

Sophie Aimon[1#], Karen Y. Cheng[1], Julijana Gjorgjieva[1,2] and Ilona C. Grunwald Kadow[1,3]

1 Technical University of Munich, School of Life Sciences, 85354 Freising, Germany
2 Max Planck Institute for Brain Research, Computation in Neural Circuits, 60438 Frankfurt, Germany
3 University of Bonn, Medical Faculty, Institute of Physiology II, 53115 Bonn, Germany
new address: Max Planck Institute for Biological Cybernetics, 72076 Tübingen, Germany

Corresponding authors: Sophie Aimon, sophie.aimon@gmail.com
Ilona C. Grunwald Kadow, ilona.kadow@gmail.com

Abstract

Movement and behavioral state influence perception, and a stimulus can elicit opposite behavioral actions depending on whether the animal is moving toward or away from it. Here, we use fast wholebrain lightfield imaging in adult *Drosophila melanogaster* to analyze the relationship between movement and neuronal activity. Using pan-neuronal calcium imaging, we observe brainwide neuronal activity that tightly correlated with spontaneous bouts of movement. Imaging of specific sets of neurons across the brain reveals that both excitatory and inhibitory as well as different types of neuromodulatory neurons are active during walk inconsistent with a reduction of inhibition on neuronal activity. While most neuron types are activated at walk-onset, serotonergic neurons show more complex patterns of activity with neurons in several brain regions being inhibited during walk. Using available anatomical data, we map forward running and turning-induced activity onto different brain subregions and sometimes individual neurons. Moreover, we find that spontaneous walk and forced walk elicit highly similar wholebrain activity suggesting that a large part of the observed activity corresponds to walk itself rather than its initiation by higher brain centers. Based on our data, we conclude that movement and movement-related sensory feedback signals originating in the ventral nerve cord induce wide-spread activity in the brain allowing the integration of behavioral state into most or all brain processes.

Introduction

Growing evidence from nematodes to mammals shows that ongoing behavior affects brain activity globally (Kaplan and Zimmer, 2020; Parker et al., 2020). Using a combination of imaging and neuropixel recordings in awake, behaving mice, recent work showed that multiple dimensions of (spontaneous) behavior, including facial or body movements, are represented brainwide, allowing the integration of external or internal stimuli with the current behavioral state (Mace et al., 2018; Musall et al., 2019; Stringer et al., 2019). Brainwide imaging at single cell-resolution of calcium activity in *C. elegans* indicated that as in mammals, multiple aspects of behavior and motor activity are represented across the brain including areas thought to be dedicated to primary sensory information processing (Kato et al., 2015). Importantly, such brainwide representations of motor states are seen independent of visual or olfactory inputs.

Previous studies suggested a similar situation in insects. For example, in *Drosophila melanogaster*, active flight modulates visual motion processing (Maimon et al., 2010). Similarly, visual horizontal system cells encode quantitative information about the fly's walking behavior independently of visual input (Fujiwara et al., 2017). Beyond primary sensory brain areas, several types of dopaminergic neurons innervating the fly’s higher brain center, the mushroom body (MB), show activity highly correlated with bouts of walking (Siju et al., 2020). Importantly, wholebrain imaging revealed that behavior-related activity occurred in most brain regions and was independent of visual or olfactory input (Aimon et al., 2019).

These and other studies provide convincing evidence for brainwide signatures of behavior across species. However, how behavior-related information is relayed to the brain, how it spreads within neural networks and what it represents remain largely unanswered questions. Different hypotheses have recently been advanced to explain the role of these large-scale activity changes: First, global activation during behavior could represent distributed motor commands. Second, global behavior-related activity could adjust sensory processing. For example, temporal integration of sensory information could be adjusted to movement speed or direction. Third, brain activity could mainly keep track of the differences between expected/intended and unexpected/unintended stimuli and outcomes and use this information to adjust behavior accordingly. In this case, whether or not a behavior leads to the immediately expected feedback from the environment could elicit very different brain signatures (Friston, 2005; Keller and Mrsic-Flogel, 2018).

Complementary to other animal models, the fly provides opportunities to study adult, global brain states associated with behavior at high temporal and spatial resolution due to its small brain size (Aimon *et al.*, 2019). In addition, recent electron microscopy (EM) connectomics has opened the path to mapping neural networks across the entire brain (Scheffer et al., 2020). Adult *Drosophila* behavior has been studied in detail for many years (Berman et al., 2016; Calhoun et al., 2019; DeAngelis et al., 2019; Geurten et al., 2014; Katsov et al., 2017; Mendes et al., 2014; Mueller et al., 2019; Tao et al., 2019; Tsai and Chou, 2019), but the resulting or underlying brain activity for even just roughly defined behavioral states such as resting or walking remains largely unknown.

Movement in adult *Drosophila* is thought to be controlled by descending neurons connecting the brain to the ventral nerve cord (VNC) which contains local pattern generators (Bidaye et al., 2020; Bidaye et al., 2014; Emanuel et al., 2020; von Philipsborn et al., 2011; Zacarias et al., 2018). This top down view is challenged by other studies suggesting that behavioral control is decentralized with feedback loops involving the brain (Schilling and Cruse, 2020), or even that many behaviors could be locally controlled by neurons in the VNC without involving the brain [e.g. decapitated grooming (Sims et al., 2019)].

Here, we use fast wholebrain imaging during ongoing walk, turn and rest to unravel the relationship between movement and neural network activity across multiple brain structures. We first identify aspects of the behavior encoded by distinct anatomically and functionally defined neural substrates. We next characterize the timing of activation at the behavior transitions between rest and walk and find that most walk-related activity happens after the transition. This is consistent with the hypothesis that global brain activity originates primarily from proprioceptive feedback rather than from top-down movement control. We test this hypothesis by comparing the activity during forced and spontaneous walk and find them to be highly reminiscent. Our results suggest that specific movement states elicit a global change in brain state thereby allowing the efficient integration of external information with ongoing behavioral actions to guide appropriate next decisions possibly leading to learning.

Results

Whole brain imaging reveals broad activation during walk

To image wholebrain activity during ongoing behavior, we fixed the fly's head to a holder and opened the posterior head capsule while leaving the legs free to move (Woller et al., 2021) (Fig. 1A). As a walkable surface, we used an air-supported ball for precise measurements of the fly's virtual trajectory (Sayin et al., 2019; Seelig et al., 2010)(Fig. 1A). In addition, given that air-supported balls can show erratic movements due to turbulences that could cue the fly to change its behavior (DeAngelis *et al.*, 2019; Sen et al., 2019), or impose constraints on the animal's posture, we performed parallel experiments with an unsupported styrofoam ball held by the fly (see Methods). We also carried out experiments without a walking substrate to compare activity related to walking to activity related to flailing movements, where the fly moves its legs freely in the air. We expressed GCaMP pan-neuronally (e.g. *nsyb-gal4;UAS-GCaMP6m*) and imaged calcium transients as a proxy of neuronal activity in the whole brain using fast lightfield microscopy (LFM) as described previously (Aimon *et al.*, 2019). Briefly, a multilens array captures an image of the entire brain. This raw image is further processed and corrected for movement artifacts to identify the brain regions or activity components with movement-correlated calcium increases (Fig. 1A).

In order to compare periods of rest with periods of spontaneous walk, we combined behavioral movies and z-projections of whole brain data (Video 1). We observed a strong increase in neuronal activity across the brain during bouts of walking compared to during resting or grooming (Fig. 1B). While LFM allows for very fast imaging frame rates (200 Hz for the whole brain), the frame rate was limited by the signal to noise ratio for specific flies and was thus adjusted for each experiment. Interestingly, we found no significant difference between the R^2-values, which indicate how well the observed brain activity can be explained by a specific behavior, for walk at different frame rate (5 – 98 Hz) for flies expressing GCaMP6f pan-neuronally (Fig. S1A). This suggests that the brain represents walking behavior at different time scales. Thus, we pooled these data for all further analysis.

In experiments where the fly was both walking and grooming, the first principal component (PC1) of the whole brain activity data was strongly correlated to walk (Fig. 1C). By aligning whole brain imaging data to an anatomical template using landmark registration, and by averaging activity in each anatomically defined region (see Methods), we also found that the activity of most regions correlated with walking (Fig. 1B). Importantly, neuronal activation

followed movement bouts at high temporal precision inconsistent with activity generated by general arousal, which we would not expect to precisely follow such bouts.

We next mapped the differences in activity during walk, flail or groom to understand their spatial organization. While we still observed an increase in activity during bouts of flailing, the brain was not as globally activated as during walking (Fig.1D and E). Strikingly, unlike grooming, which resulted in local activation ventral brain areas consistent with (Hampel et al., 2015), and flailing, the large majority of brain regions were highly correlated with walking (Fig. 1D and E). Indeed, using walking behavior we were able to explain ~ 20 % of all variance observed in the experiments (R^2 median = 0.194, Fig. 1E).

To make sure our results were not biased by inhomogenous expression in the pan-neuronal transgenic driver line, we used two different lines (*nsyb-Gal4* and *GMR57C10-Gal4*). A linear model (Table 1) showed that there was no significant effect of the Gal4-driver. We found a small but significant effect of the GCaMP version used, however, and thus used a model to take this small effect into account for the rest of the study (see Methods). Using this model we quantified the effect of the distinct brain regions on both the normalized coefficient and the R^2 of the regression with a behavior regressor (Fig. 1G, S1B-F). While all brain areas are significantly activated during walk (Fig. 1G, S1B), only the region of the GNG shows strong activation during grooming (Fig. S1F). Flailing represents an intermediate state with many brain regions activated but to a lower degree and less consistently as compared to walk (Fig. 1E, S1C,E).

To test whether part of the observed global brain activity could be due to visual input coupled with the behavior, e.g. by the fly seeing the optic flow from the ball (Borst et al., 2020; Suver et al., 2016), or unexpectedly fixed reflections from the environment (Creamer et al., 2018), we performed the same experiments but covered the fly's eyes with black nail polish to prevent outside light from activating its photoreceptor neurons. With such strongly limited visual input, we still observed a very similar, not significantly different, global activity pattern indicating that visual input is a minor contributor to the observed wide brain activity (Fig. 1F). This also suggests that the global increase in activity during walk is not due to a mismatch between an actual and a predicted visual stimulus.

Together these data show that walking behavior induces a change in global brain activity with most brain regions showing highly temporally correlated activity during bouts of walking.

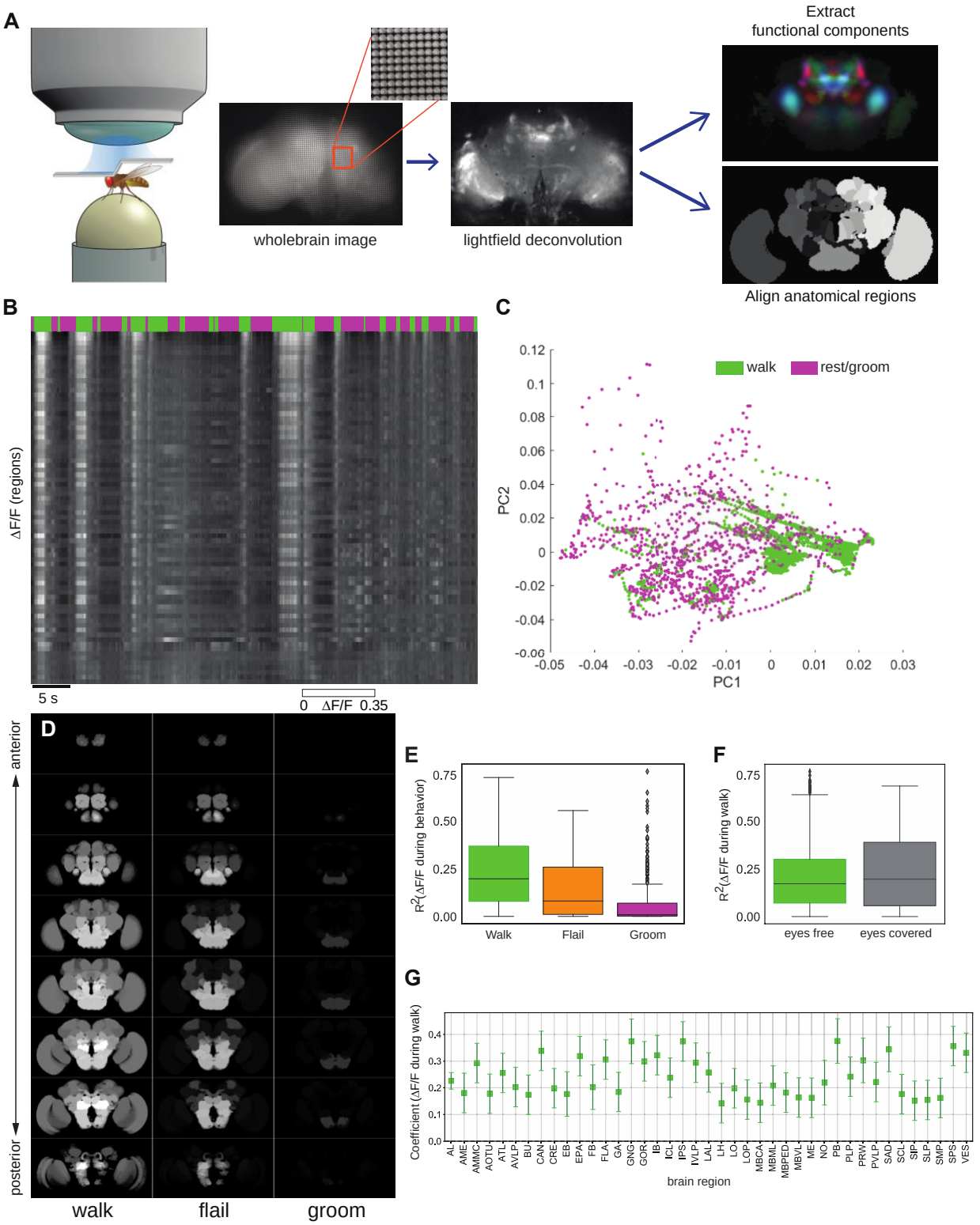

Figure 1: *Global brain activation during walk. (A) Schematic overview of the preparation and analysis method. Please see methods for details. (B) Raster plot of the activity of regions. Top panels depict walking bouts in green and rest or grooming in magenta. Lower panel shows calcium activity elicited throughout the experiment. The brighter the higher*

the calcium transients. (C) First two principal components from whole brain activity color-coded with behavior. (D) Z-stack map of R^2 median (Walk: N=16, Flail: N=7, Groom: N=6) for regression between regional activity and walk, flail or groom. (E) R^2-value of regression coefficients at different behavioral conditions (all regions were pooled, but p-values are obtained after averaging regions for each fly. Walk: N=16, Flail: N=7, Groom: N=6). P-values: Walk vs. Flail 0.085,

Walk vs. Groom: 0.011, Flail vs. Groom: 0.26 (F) R^2-value of regression coefficients for walking with eyes free (not painted, N=5) and eyes covered (painted, N=5, p-value: 0.34). (G) Normalized coefficient of different regions' activity regression with walk. All regions' 95% CI are above zero. N=16.

***Video 1**: Movie of pan-neuronal activation during walk and groom (accelerated).*

***Table 1**: ANOVA analysis of regression R^2 for brain activity vs. different types of behavior and for different pan-neuronal expression genotypes*

Both inhibitory and excitatory neurons are recruited during walk

To gain more insight into the type of neurons responsible for the global state change of the brain during walk, we expressed GCaMP in different types of neurons and repeated the experiment as described above. It is conceivable that broad brain activation arises due to a disinhibition occurring specifically during periods of walking (Benjamin et al., 2010). To address this possibility, we expressed GCaMP6m exclusively in GABAergic inhibitory neurons using the GAD1-gal4 driver. We also did the same with a driver for glutamatergic neurons (*Vglut-gal4;UAS-GCaMP6m*) as glutamate is thought to be inhibitory in the fly. In addition, we analyzed activation patterns during behavior in excitatory neurons by imaging from all cholinergic neurons in the fly brain (*Cha-gal4;UAS-GCaMP6m or UAS-GCaMP6f*). Using the same approach and analysis as described above, we detected an increase in global brain activation, which again correlated highly with walking bouts, for excitatory and inhibitory types of neurons (Fig. 2A).
As for the pan-neuronal data, we mapped this activity to all brain regions to create a functional map of activity during walk (Fig. 2B,C). Among other regions, we found that the gnathal ganglia (GNG) and the antennal mechanosensory and motor center (AMMC), known to be important for leg coordination (Emanuel *et al.*, 2020), responded to walk for all genotypes (Fig. 2B,C). Using a linear regression model, we determined that similar to the pan-neuronal data, excitatory neurons labeled by Cha-Gal4 were activated in all brain regions (Fig. 2D, S2A). We observed highly similar activation patterns with neurons labeled by Vglut-Gal4 and GAD-Gal4 being significantly activated during walk (Fig. 2E,F and S2B,C). Brain regions such as the protocerebral bridge (PB), the cantle (CAN), the vest (VES) and the superior posterior slope (SPS) were correlated especially strongly in all three types of neurons (Fig. 2D-F).
Together these data show that inhibitory neurons as well as excitatory neurons are activated in all brain regions during walking. Moreover, these data suggest that the observed activity in pan-neuronal imaging is not mediated by a global disinhibition in the brain, but rather a result of a combined activation of different types of neurons, including excitatory and inhibitory neurons.

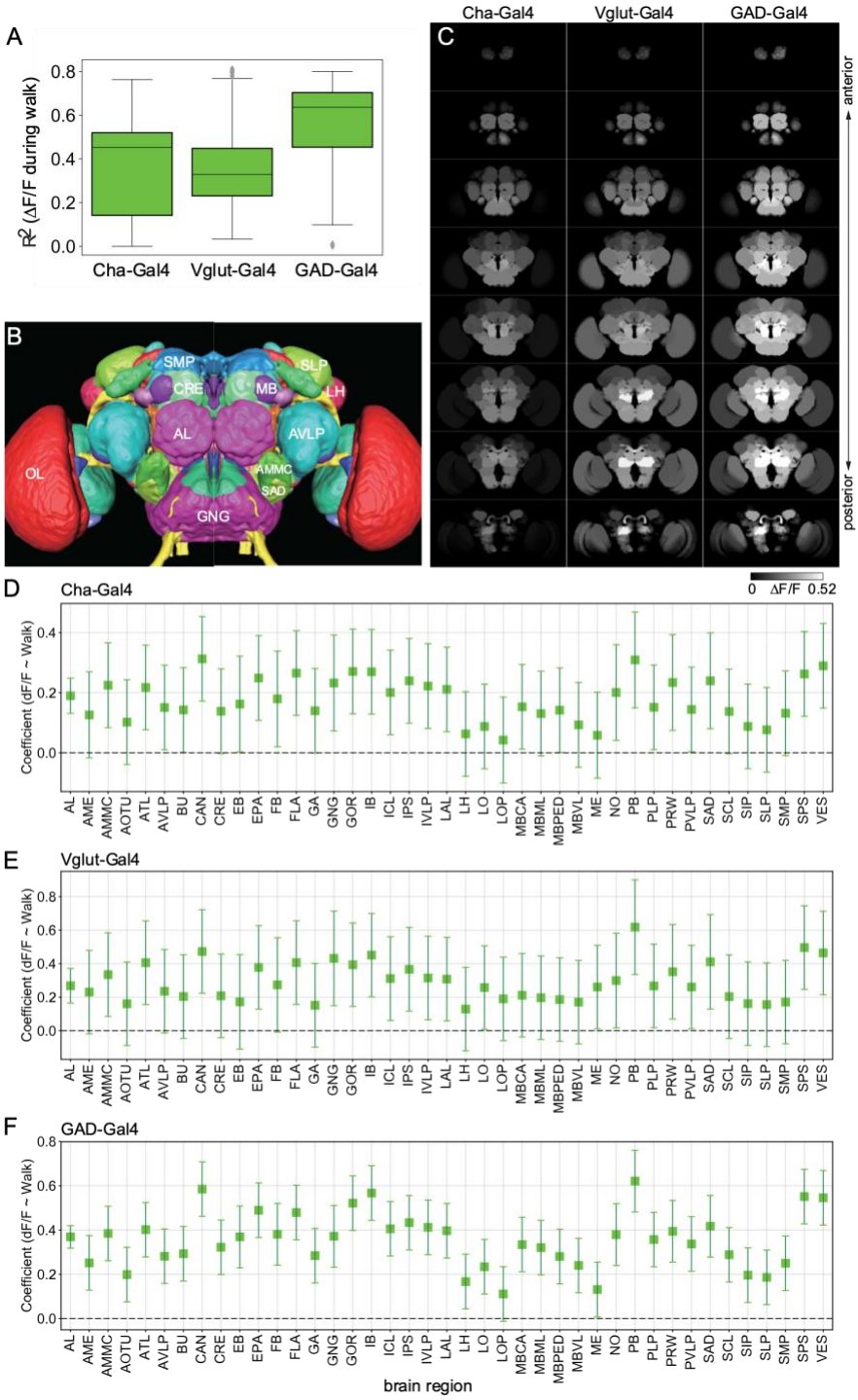

Figure 2: *Activity of neurons releasing the three major neurotransmitters, glutamate, GABA and acetylcholine during walk. Data for each Gal4 genotype has N=5 flies. (A) R^2 for behavior regression at different conditions (all regions were pooled). No pairwise comparison is significantly different. (B) Overview of major brain regions as defined in (Ito et al., 2014). (C) Activity maps (regression coefficient) of functional regions activated during walk for Cha-gal4, GAD1-gal4 and Vglut-Gal4 expressing neurons. (D) (E) and (F) Coefficient during walk for different brain regions and*

95 CI, for Cha-Gal4 expressing excitatory neurons (D), Vglut-Gal4 expressing inhibitory neurons (E) and GAD-Gal4 expressing inhibitory neurons (F).

Aminergic neuron activity is strongly correlated with behavior

Monoamine-releasing neuromodulatory neurons, i.e. dopamine, serotonin and octopamine (the fly's equivalent to mammalian noradrenaline) have been shown in the past to be important to control and adjust behavior (Emanuel *et al.*, 2020; Li et al., 2017). However, the role of these neuromodulators during motor behavior remains to be fully elucidated.

Previous data suggested that both walking and flailing, but not grooming or resting, were related to an increase in dopaminergic neuron activity (DAN) (Aimon *et al.*, 2019; Siju *et al.*, 2020; Zolin et al., 2021). We used different Gal4 drivers for different types of neuromodulatory neuron i.e. Tdc2-Gal4/octopamine, Trh-Gal4/serotonin. For dopamine, we combined TH-Gal4 with DDC-Gal4 or GMR58E04-Gal4 to cover all dopaminergic neuron types (Cohn et al., 2015; Siju *et al.*, 2020).

While we observed an increase in activity for all neuromodulatory neuron types, serotonergic neurons were significantly less activated than dopaminergic and octopaminergic neurons (Fig. 3A, Video 2-4). We again also mapped the activity to the regions of the brain (Fig. 3B). Contrary to results shown above with pan-neuronal and broad neurotransmitter lines, maps were distinctly patterned for the individual aminergic lines, as revealed by overlaid activity maps (Fig. 3C).

In addition to the mushroom body (MB), most regions were consistently activated in neurons expressing GCaMP6m or GCaMP6f under the control of TH/DDC-Gal4 (Fig. 3B-D, S3A). Importantly, besides the neurons that were already implicated in prior work (Aimon *et al.*, 2019; Cohn *et al.*, 2015; Liu et al., 2012; Siju *et al.*, 2020), whole brain imaging suggested that many additional DANs were activated during or due to movement (Fig. 3A-C). Octopaminergic neuron activity (imaged with *Tdc2-gal4;UAS-GCaMP6s*) was also highly correlated with walking (Fig. 3A,B). The activation was particularly high for neurons located or projecting into the ventromedial neuropils (VMNP, Fig. 3B,C,E and S3B).

Using whole brain imaging of serotonergic neuron activity (*Trh-gal4;UAS-GCaMP6m,f or s*), we found that the activity of several regions was highly correlated with walking (Fig. 3A,B). Surprisingly though, the strongest correlation was negative and mapped to the anterior ventrolateral protocerebrum (AVLP) region (Fig. 3B (blue area), 3F). This suggested that while some populations of serotonergic neurons were activated, some subsets, in particular in the

AVLP, were inhibited with walk (Fig. 3F, S3C). Overlaying activity maps between Trh-Gal4 neuron activity and TH/DDC-Gal4 or Tdc2-Gal4 neurons revealed again that walk activates different types of neuromodulatory neurons in different brain regions (Fig. 3C).

Together, these data show that walking behavior activates, and in some cases inhibits, all main types of aminergic neuromodulatory neurons in various but distinct brain regions. Thus, the observed pan-neuronal global activity during walk is a result of the activation of excitatory, inhibitory and neuromodulatory neuron responses to walk.

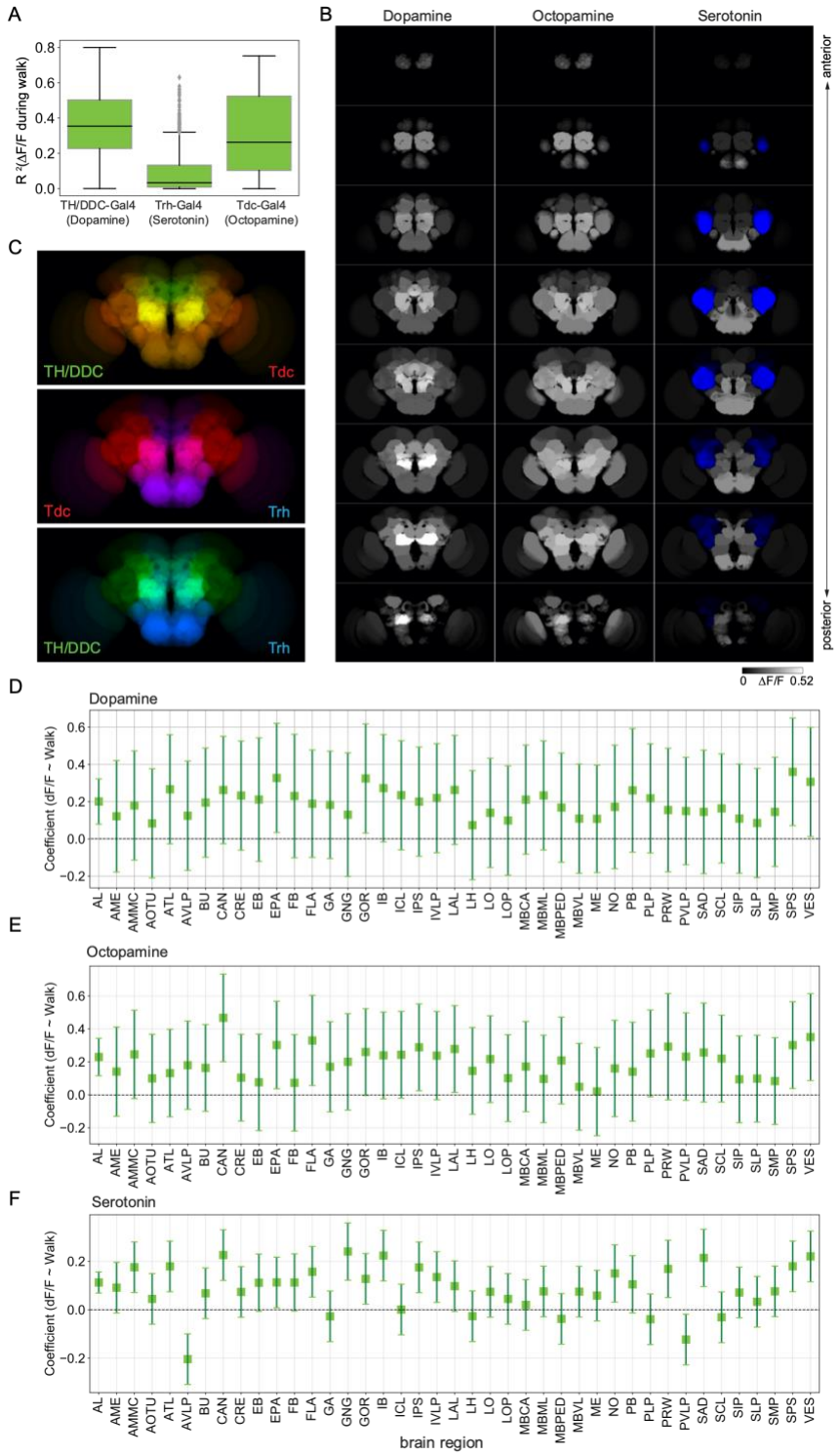

Figure 3: *Neuromodulatory neurons are strongly and differentially activated during walk. TH: N=9, TDC: N=7, Trh: N=6 flies. (A) Coefficient of determination for behavior regression at different conditions (all regions were pooled). P-values: TH vs. Trh: 0.032, TH vs. TDC: ns, Trh vs. TDC: 0.040 (B) Activity maps (regression coefficient) of functional regions activated during walk for TH-gal4 and DDC-gal4 or GMR58E04-Gal4 (dopaminergic neurons), TDC2-gal4 (octopaminergic neurons) and Trh-Gal4 (serotoninergic neurons) expressing neurons. Blue indicates inhibition. (C)*

Overlay of activity maps of two neuromodulators in each panel. (D) Coefficient during walk for different brain regions for TH/DDC-Gal4 expressing dopaminergic neurons. All regions are significantly correlated. (E) Coefficient during walk for different brain regions for Tdc2-Gal4 expressing octopaminergic neurons. All regions are significantly correlated. (F) Coefficient during walk for different brain regions for Trh-Gal4 expressing serotonergic neurons. All regions are significantly correlated.

Video 2: *Movie of TH/DDC-neuronal activation during walk (accelerated).*
Video 3: *Movie of TDC2-neuronal activation during walk (accelerated).*
Video 4: *Movie of Trh-neuronal activation during walk (accelerated).*

Wholebrain activity data identifies specific brain regions or even neurons

Global brain activity can be used to generate functional maps of the brain (i.e. fMRI). While such data can be generated for other animals including humans, the fly (along with *C. elegans* and in the near future zebrafish) currently provides the important advantage to combine such activity maps with highly detailed anatomical maps from light microscopy with cellular resolution and from recent whole brain EM connectomics with synaptic resolution. Ultimately, such data could be used to generate precise models of how recorded neural activity spreads through a brain.

As a first step we adjusted the region classification used above to better match our functional data to smaller brain regions or ideally single neuron types (Chiang et al., 2011; Lee et al., 2020). To this end, we extracted functional regions using PCA followed by ICA to unmix the PCA maps (see Methods) (Fig. 4A, S4A-C). We grouped small functional regions within a larger brain area (e.g. different antennal and protocerebral bridge glomeruli), if the precision of the alignment of the template did not allow a clear assignment of individual regions. Interestingly, almost all functional components derived from recorded neuronal activity matched previously identified anatomical structures without further subdivisions or blurring of anatomical boundaries. A few exceptions stood out: for example our functional data separated the larger region of the AVLP into smaller subregions (Fig. 4A, S4B, orange box) suggesting that subregions of the AVLP had different activity signatures.

Not all components were correlated with walk, representing onging activity unrelated to walk. Among the components correlating with walk, the PENP-SLP (periesophageal neuropils and superior lateral protocerebrum) and PENP-CL (periesophageal neuropils and clamp) components might contribute to relaying the information that the fly walks from the ventral neuropils (e.g. GNG) to higher areas. The WPNb component (likely generated by the WPNb

neuron (Coates et al., 2020)) was weakly correlated with walk but had a R^2-value significantly above zero and could thus also relay the activity to higher regions.

In addition to the data collected for the data collected with pan-neuronally expressed GCaMP, we used the same analysis pipeline to assign functional components to the data collected for inhibitory, excitatory and neuromodulatory neurons (Fig. 4A). For dopaminergic neurons, walk-correlated neuronal activity was found, for instance, for components in and around the MB (i.e. γ3-compartment as previously observed; (Cohn *et al.*, 2015; Siju *et al.*, 2020; Zolin *et al.*, 2021), in the central complex (protocerebral bridge (PB) and ellipsoid body (EB), but also in ventral neuropil such as the WED and neuropil connecting central regions to the optic lobes (Fig. 4A). For octopamine, one particular component connecting the optic lobe and the periesophageal neuropil was correlated strongly with walk, the OL-PENP, while for serotonin the highest R^2-value was detected for the AVLP and components within (Fig. 4A).
Interestingly, most components with significant R^2-values were positively correlated with walk with one exception (Fig. 4B,C): a component of the AVLP, a region we named the AVLP shell due to its shape, was negatively correlated with walk, i.e. was inhibited during walk (Fig. 4B). As this component was mostly detected in experiment using Trh-Gal4, serotonergic neurons were likely responsible for the decrease in activity during walk (see also Fig. 3).

Several of these components were previously implicated in walking behavior or its modulation, many others were not (Table 2) indicating that whole brain imaging during behavior in combination with our analysis pipeline provides a powerful method to pinpoint new brain regions and neurons involved in the control of or response to walking behavior.

Table 2*: List of all reproducibly identified components correlated with walk and additional information including putative neurons.*

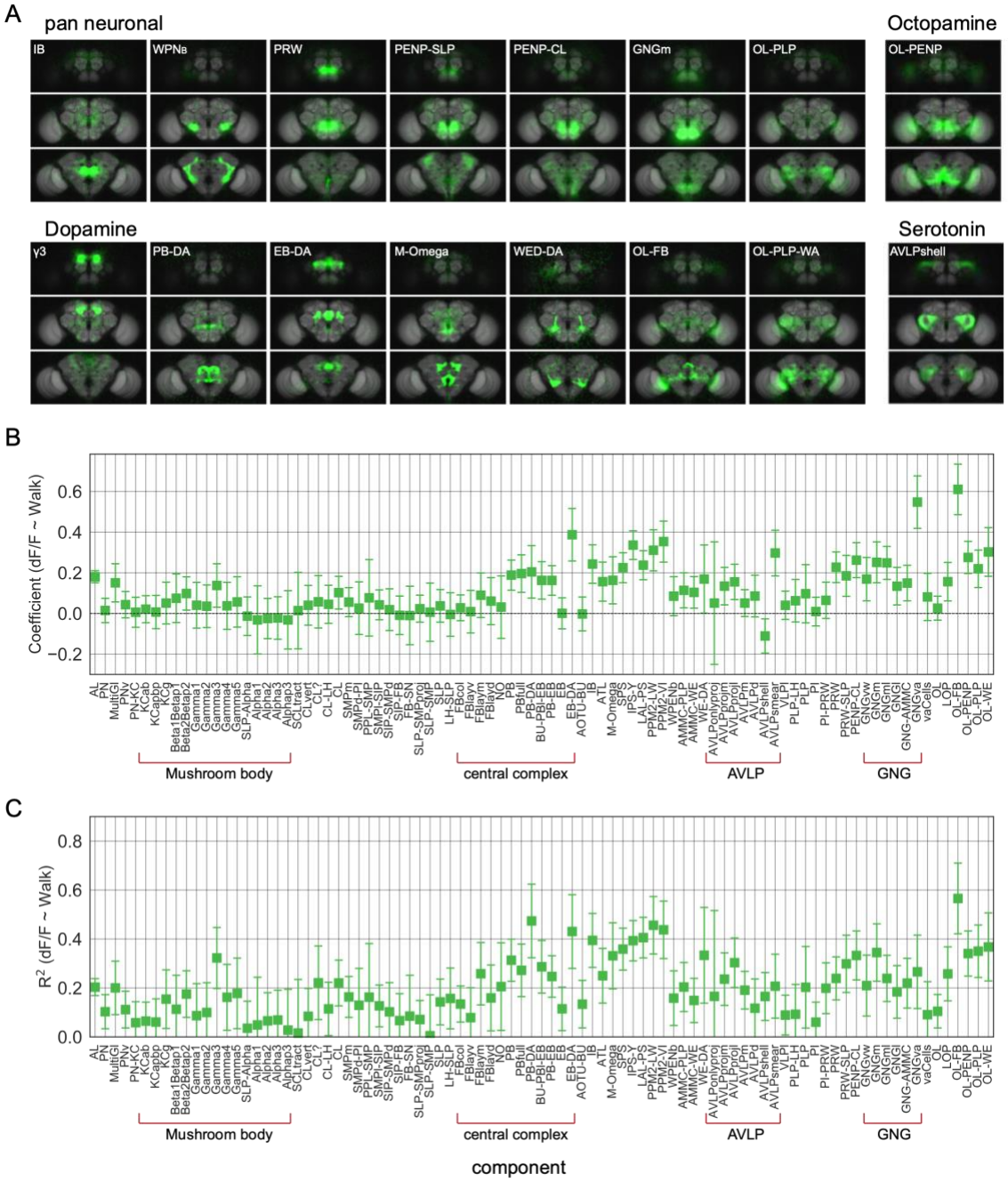

Figure 4: *Whole brain analysis pinpoints specific subregions responding to walk. (A) Images of example components that are significantly correlated with walk (Coefficient or R^2 95% CI above zero). Upper left: components derived from imaging with a pan-neuronal driver. Upper right: components derived with Tdc2-Gal4. Lower left: components derived with TH/DDC or GMR58E02-Gal4. Lower right: components derived with Trh-Gal4. (B) Correlation coefficient for components activity vs walk. (C) R^2-values for components activity vs walk.*

Turning activates specific brain regions and neurons

Some functional regions activated during behavior showed an activity that appeared to be mirrored by the other half of the brain (Fig. 5A). We next asked whether these regions had differential activity when turning left or right (Fig. S5). We found that the components that correlated with turning were reproducibly found across different flies based on similar position and morphology (Fig. 5A for examples in *TH/DDC-Gal4;UAS-GcaMP6m*). These included the IPS-Y and LAL-PS as described in a previously (Aimon *et al.*, 2019). For dopaminergic neurons, the components most correlated with turning could be matched with specific neurons such as neurons of the PPM2 cluster, i.e. PPM2-LW (PPM2-LAL-WED: PPM2- lateral accessory lobe-wedge (Mao and Davis, 2009))(Fig. 5A, right panels; Video 5). By subtracting the coefficient of activity on the contralateral side from the coefficient on the ipsilateral side, we found that some of these turning components were not active at the same time in both brain hemispheres, but instead were activated differentially depending on whether the fly turned left or right (Fig. 5B).

These data show that part of the globally observed increase in neuronal activity during walking corresponds to turning behavior and likely other behaviors that we have not dissected for this study. Nevertheless, the presented method can pinpoint individual neurons active during a distinct behavior such as turning. Future work will aim at mapping additional behaviors or distinct behavioral syllables to their corresponding functional and anatomical components in the brain.

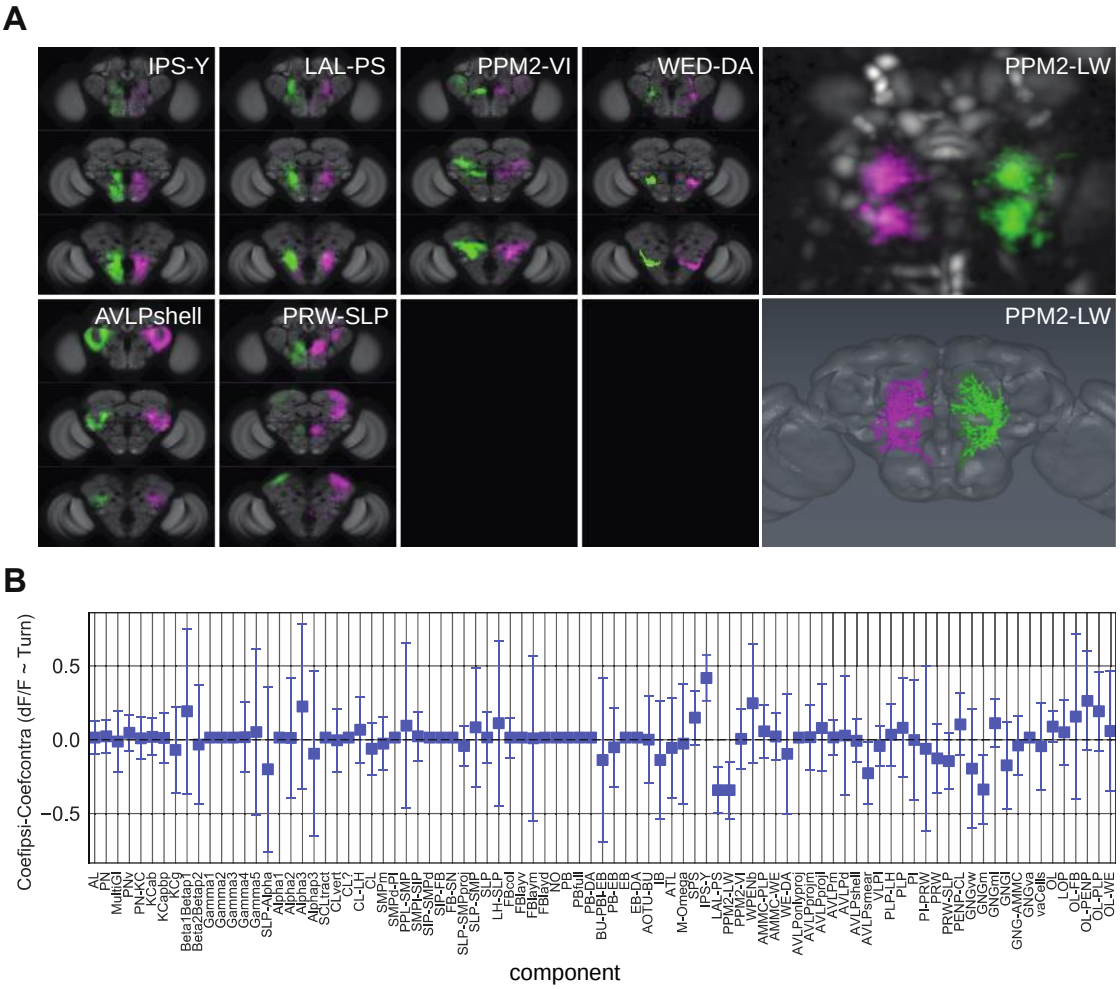

Figure 5: *Turning activates specific components and neurons. (A) Examples of components present in both the left and right hemisphere labeled in different colors (magenta and green). Panels on the right present an example component that could be mapped to a single neuron. Upper right panel: Turning-correlated component, lower right panel: reconstruction of neuron that this functional component was mapped to. (B) Difference between correlation coefficient for turning on the ipsilateral side minus the coefficient on the contralateral side is displayed as a function of the identified components. Positive and negative correlations correspond to components being active more during turn on the ipsi-lateral side than the contra-lateral side and the reverse, respectively.*

Video 5*: Video sequence showing activation of the PPM2-LW neurons during turning.*

Brain dynamics at transitions between rest and walk

So far, we have analyzed the activity during walk, turn, flail, groom or resting. Next, we analyzed whole brain activity at the transition between behaviors. As the observed increase in activity appeared during walk, we focused on the transition between rest and walk. Importantly, different GCaMP versions showed equally fast, non-distinguishable onset dynamics. We thus computed the cross-correlation between the activity of the components and the onset of walk (with a maximum of +/- 200 ms time shift due to lower recording speed in several samples with low signal-to-noise ratio, Fig. S6A). Walking-related changes in brain activity occurred immediately after walk onset in many components such as the MB-γ3 and 4 compartments, different components in the GNG or the PB (Fig. 6). By contrast, other components including the α2-Kenyon cells (KC) or the olfactory projection neurons (PN) showed very little change at walk onset (Fig. 6). A few components such as the AVLPshell, SLP-SMP, α3-KCs, α'3-KCs, and layer 5 of the fan shape body (FBlayV) showed a decrease in activity with walking onset and possibly slightly before (Fig. 6). Several other components displayed more variable dynamics and at times too variable between flies to detect a clear trend.

To further investigate putative differences in dynamics between neuron types, we next investigated the timing of neuromodulatory, inhibitory and excitatory neuronal activity separately relative to walking onset in different brain regions (Fig. S6). First, we analyzed the activity of cholinergic neurons (Cha-Gal4) relative to the start of walking (Fig. S6A). We saw a significant and strong increase in normalized fluorescent activity of the GCaMP indicator in all brain regions (Fig. S6A). Interestingly, in the majority of brain regions, this activity appeared to increase just before or at walk onset (Fig. S6A). Activity before walk onset could be due to preparatory movements that were not detected as walk (Ache et al., 2019). The activity of glutamatergic, inhibitory neurons appeared to be more variable between regions as compared to the activity of cholinergic neurons with some brain regions showing activity at walk onset and some milliseconds before (Fig. S6B). Nevertheless, GABAergic neurons showed by and large the same activation patterns as cholinergic neurons with a significant increase in activity at walk onset (Fig. S6C). These data confirm our earlier conclusion and indicate that inhibitory and excitatory neurons in essentially all brain regions are activated when and after the fly starts to walk.

Given the suggested importance of DANs for movement preparation and initiation in vertebrates (Azanchi et al., 2013), we next analyzed DAN activity more carefully (Fig. S6D). In many brain

regions, DAN activity increased at the start of walk (Fig. S6D). In others such as the MB vertical lobes (MBVL), the activity went up before the fly started to walk and stayed high during walk (Fig. S6D). Some changes in activity occurred after the initiation of walking in octopaminergic neurons (OAN) (Fig. S6E). In most regions, OANs became activated at or just after walk onset displaying an overall very similar picture as seen for cholinergic or inhibitory neurons (Fig. S6A-C, E). This was consistent with a study showing a role for octopamine in flight initiation and maintenance (Brembs et al., 2007). We observed the most interesting and complex activation patters for serotonergic neurons in different brain regions (Fig. S6F). First, we observed a decrease in activity at walk onset for several brain regions including the AVLP, the PLP, MB calyx (MBCA) and the ICL. However, some regions showed a clear increase at walk onset (e.g. GNG, saddle (SAD) or SIP) (Fig. S6F). We also saw regions where the activity increased initially but decreased quickly after walk onset (e.g. LAL) (Fig. S6F).

While we currently do not understand the biological significance of these different activation patterns in different brain regions, our data suggest that the global change in brain activity elicited through walk represents a complex pattern of neuronal activities of individual neurons types or individual neurons. However, the bulk of the activation occurred just after walk onset, suggesting that walking behavior itself induces a global brain change rather than the reverse.

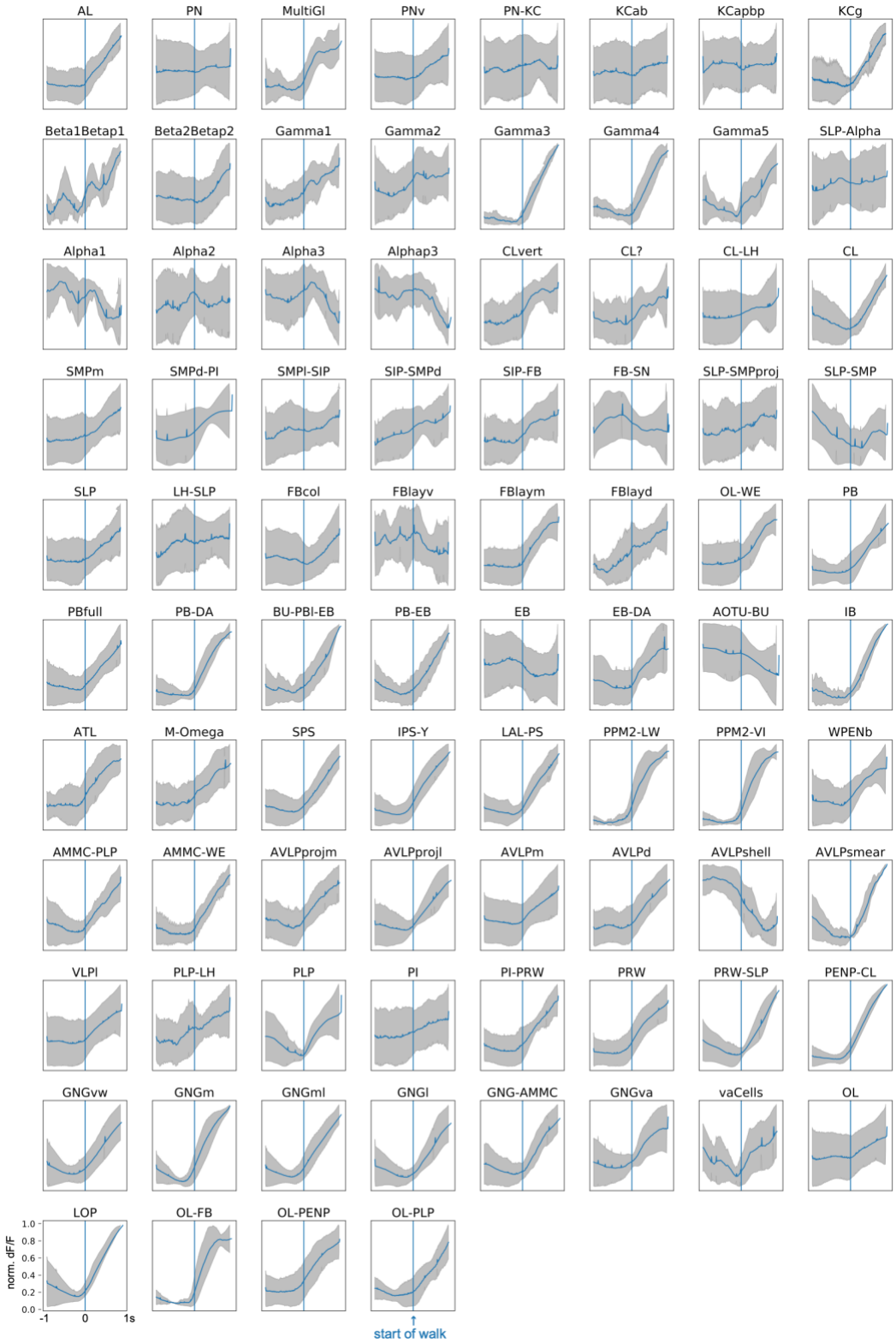

Figure 6: *Walk induces activity in multiple functional components across the brain at start of walk. Walk-onset triggered average activity for pan-neuronal data in individual active components. Note that most regions are activated after walk onset. See Table 2 for definition of acronyms.*

Forced walk and forced turning recapitulates most activity

Our data suggest that walking induces a change of activity in most of the brain. But where does this activity come from? We hypothesized that in the extreme case, activity could essentially originate from two opposite sites. First, the activity could arise initially in superior decision making areas and then spread across the brain (top-down) or, second, activity is initiated by motor activity and proprioception (bottom-up) and then distributed to higher brain areas. In the latter case, the activity would originate in the ventral nerve cord (VNC) and move to the basal regions of the brain, i.e. the GNG, via ascending neurons (Tsubouchi et al., 2017). Aligning the onset of GCaMP fluorescence increases to the onset of walk suggested that few regions, among them the GNG, appeared to be activated slightly before the majority of the brain regions responding to walk (Fig. S6A).

We thus asked whether the walk-induced activity seen in the GNG could indeed be contributed by axon terminals of ascending neurons. To this end, we expressed a synaptically-tethered GCaMP, syt-GCaMP6, under the control of a pan-neuronal driver and imaged whole brain activity during walk (Fig. 7A). Compared to cellular-GCaMP, syt-GCaMP activity was very strong in the GNG, AMMC and AVLP, the regions receiving input from the VNC (Fig. 7A) (Tsubouchi *et al.*, 2017).

Since such axonal activity, or a fraction of it, could potentially also originate from top-down projections, we carried out another experiment and compared spontaneous, self-induced walk to forced walk (video 3). We argued that if the broad activation indeed comes from proprioception of walking or related sensory input from the legs, we should also observe a global activation when the fly is forced to walk rather than decides to walk spontaneously. To test this idea, we placed a walking substrate controlled by a motor under the fly legs (see Video 6 and methods). We forced the flies to walk by turning this motor on and off. Spontaneous walk in these flies elicited the typical wholebrain activity as described above (Fig. 7B,D). Remarkably, forced walk also induced a highly similar activity across the brain (Fig. 7C,D, Video 6). Indeed, we found no significant difference in the correlation coefficient or the R^2-value and regression coefficients across different functional components during spontaneous as compared to forced walk (Fig. 7E,F). In addition, flies with a surgically severed connection between brain and VNC showed hardly any activity in the brain during forced walk (Fig. 7D, Video 7) consistent with the hypothesis that whole brain activity is induced by walk itself and originates in the VNC.

Importantly, these observations were not only true for pan-neuronal data but also for dopaminergic, octopaminergic and serotonergic neuronal subsets (Fig. S7A-F). While we did observe some variation between forced and spontaneous walk in correlation coefficient or R^2-value for walk, no significant difference was found for any of the brain regions (Fig. S7A-F) further suggesting that walking, whether spontaneous or forced, elicits a highly similar global state change of the brain.

Taken together, these data are consistent with a model wherein a substantial part of the whole brain activity observed during walk is induced by walk itself and/or by walk-related proprioceptive stimulation and not by top-down activity of higher brain centers. As we did not observe a stronger increase in overall brain activity during forced walk as compared to spontaneous walk, our data also suggests that brain activity does not represent a mismatch, or error signal, between actual and predicted proprioceptive feedback.

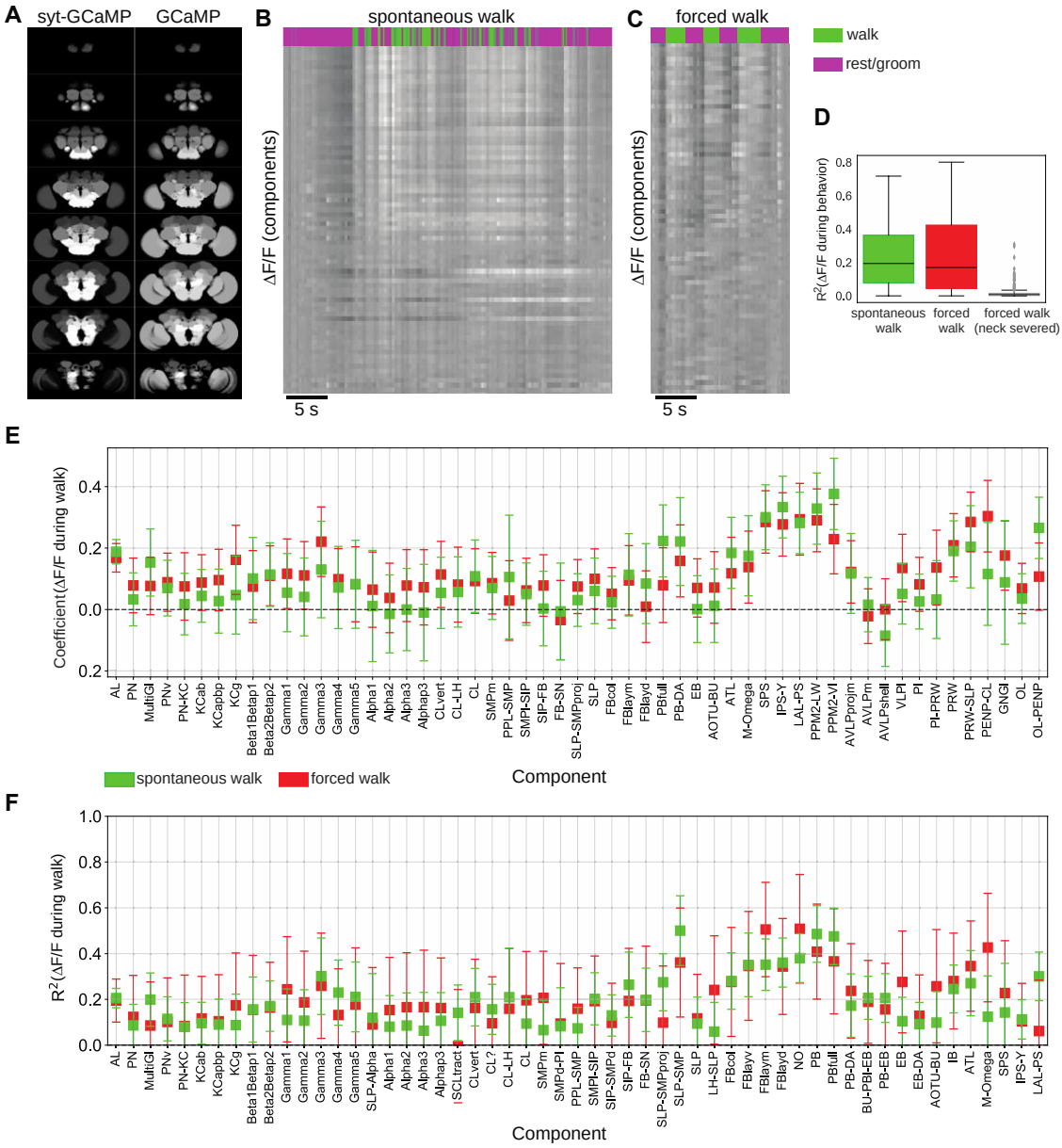

Figure 7: *Forced and spontaneous walk elicit highly similar whole brain activity. (A) Z-stacks of map of brain regions activated by walk in flies expressing cytosolic GCaMP (pan-Gal4;UAS-GCaMP6m) or synaptically tagged GCaMP (pan-Gal4;UAS-GCaMP6m) (B) Time series of active components during spontaneous walk or rest (magenta vs. green). (C) Time series of active components during forced walk or forced rest (magenta vs. green). (D) Coefficient of determination for behavior regression at different conditions (all regions were pooled, spontaneous, forced, forced with severed connection between VNC and brain) (E) Correlation coefficient for walk in different functional components. No significant difference was detected between forced and spontaneous walk. (F) Coefficient of determination for behavior regression for different active components for forced vs. spontaneous walk.*

Video 6: Video showing whole brain activity of a fly being forced to walk on a rotating rod.

Video 7: Video showing whole brain activity of a fly with a severed connection between brain and VNC being forced to walk on a rotating rod. Note that the fly is still capable of walking on the rod when being forced. We did, however, not observe spontaneous walking activity.

Discussion

Work over the last years has revealed that locomotion and movement influence the activity of neurons in many brain areas and organisms (Busse et al., 2017; Kaplan and Zimmer, 2020). Importantly, motor activity modulates not only local activity in specific brain regions, instead it appears to change the global state of the brain. Where this activity originates from, how it spreads, and what it means for the animal is still debated (Kaplan and Zimmer, 2020). Using a tethered fly preparation and fast *in vivo* whole brain imaging, we showed that movement elicits a global change in brain activity during spontaneous as well as forced walk. Our data further suggested that walk activates several different classes of neurons including excitatory (cholinergic) neurons, inhibitory neurons as well as aminergic, modulatory neuron types. With the exception of serotonergic neurons which are inhibited during walk in some brain areas, we observed neuronal activation across all brain regions at the start of and during walking, but not during grooming or resting. Using PCA/ICA transformation, we mapped neuronal activities to discrete functional components, which we assigned to specific smaller subregions and in some cases even to single neurons by aligning the activity data to a comprehensive set of anatomical images and data from different community sources. For instance, we pinpointed specific neurons activated during turning. Based on our data and analysis, we propose that locomotion activates the brain by sending movement and proprioceptive information to the base of the brain (the GNG) from where it activates all brain regions. These data and analysis inspire testable hypotheses and provide a resource of potential neural substrates involved in the perception or control of walking behavior.

Role and origin of broad activation during ongoing behavior

One important concept to explain the role of behavioral state-dependent neural modulation is referred to as ‘Active sensation’ (Busse *et al.*, 2017; Parker *et al.*, 2020). Essentially, ongoing movement can shape how neurons respond to visual, somatosensory and other sensory stimuli (Chapman et al., 2018; Cruz et al., 2021; Fenk et al., 2021; Fu et al., 2014; Haesemeyer et al., 2018; Henschke et al., 2021). Our data indicate that whole brain activity is elicited with walk onset and maintained afterwards (see Figure 6). Our analysis furthermore revealed brain areas and select neurons that respond to turning (see Fig. 5). These observations support the conclusion that movement specific, proprioceptive and other sensory information reach the brain and modulate brain activity widely. Such information could serve multiple purposes from uncoupling of sensory-to-motor information, i.e. own movement *vs.* movement of environment, to learning of complex movements. Brainwide neural and glial responses appear to enable

behavioral flexibility in zebrafish (Mu et al., 2019; Wolpert et al., 2011). By coupling sensory processing and behavior in a closed loop, brain activation during ongoing behavior could resemble a form of working memory, in part for learning to improve future (motor) behavior or to relate body-movement to environmental information (Lu et al., 2021).

Our results are most consistent with a model where proprioceptive, walking and leg sensory information are sent from the VNC into the GNG at the base of the fly's brain (Agrawal et al., 2020; Mamiya et al., 2018). This is consistent with extracellular recordings from V1 neurons of mice walking on a ball showed that evoked visual responses differed during movement as compared to neurons of still animals. Similarly, fly visual neurons respond stronger stimuli during active walk or flight (Chiappe et al., 2010; Maimon *et al.*, 2010). In these studies, and ours, visual information was not required to induce these changes during walk (see Fig. 1). So, how is walking related information relayed to the brain? Tuthill and colleagues recently identified some of the presumably many neural substrates in the VNC that receive, process and relay proprioceptive sensory information from the legs to the CNS (Agrawal *et al.*, 2020; Mamiya *et al.*, 2018). Their findings provide strong support for an important role of proprioception in movement and locomotion control in the adult fly. This information is transmitted by ascending neurons from the VNC to the central brain. So far, relatively little is known regarding the type, connectivity and function of the likely dozens or more ascending neurons in *Drosophila*, but screening approaches and advanced imaging techniques have shed light on some of them (Allen et al., 2020; Chen et al., 2018; Sen *et al.*, 2019).

While grooming or forced walk on a treadmill do not require an active brain, lesions of the neck connectives as we have carried out dramatically decrease spontaneous walking in locusts (Kien, 1990a; b) and in flies (see Fig. 7) indicating that at least initiation of walk can be dependent on the brain. Surprisingly, whole brain activity induced by spontaneous walking was similar to the activity we observed by forcing the animal to walk on a rotating rod (see Fig. 7). This result and our finding that the activity first induced by walk in the GNG stems from axons are consistent with the interpretation that walk itself and not top-down motor control is responsible for the majority of activity observed in actively moving animals' brains. We can, however, not exclude that the fly that was forced to walk responded not only with passive rhythmic walking, while also by trying to actively stop and counteract the rotating rod, but this would have engendered a modification in behavior that we did not observe.

Walk elicits differential activities in neuromodulatory neurons

Perhaps not surprisingly, neuromodulatory systems participate and show signatures of ongoing behavior in the adult fly brain (see Fig. 3). Dopaminergic and octopaminergic neurons are broadly activated when the fly walks but not when it grooms (see Fig. 3, (Aimon *et al.*, 2019; Berry et al., 2015; Siju *et al.*, 2020)), while serotonergic neurons show more complex activation patterns and timing with areas such as the AVLP being inhibited during walk (see Fig. 3 and S6).

While we do not understand the role of these neurons and their distinct activation patterns, a role in locomotion of neuromodulatory neurons holds true across species. Acetylcholine and norepinephrine/octopamine are two of the key neuromodulatory systems involved in modulation of brain state and sensory processing during locomotion behaviors in a variety of species (e.g.(Collins et al., 2021; Kato *et al.*, 2015; Parker *et al.*, 2020; Reimer et al., 2016; Tantirigama et al., 2020)). In vertebrates, basal ganglia and brainstem aminergic neurons affect the cortico-basal ganglia-thalamic loops. A disruption of these loops can result in a loss of motor control (Vicente et al., 2020). Such loops likely exist in insects, too. For example, several octopaminergic neurons connect lower brain regions to the MB (Busch et al., 2009). Dopaminergic neurons innervate central complex and MB (Mao and Davis, 2009). In line with this, we observe a strong activation of dopaminergic and octopaminergic neurons during walk.

Interestingly, serotonin differs and also shows regional decreases of activity during walk, for instance in the AVLP (see Fig. 3). This is consistent with the mixed roles of serotonergic neurons in the control of motor behavior in different vertebrate species (Flaive et al., 2020; Vitrac and Benoit-Marand, 2017). In insects, serotonin regulates various types of motor behaviors including feeding, aggression and larval locomotion (e.g. (Aonuma, 2020; Helfrich-Förster, 2018; Hsu and Bhandawat, 2016; Ngai et al., 2019; Schoofs et al., 2018; Schoofs et al., 2014)). The AVLP receives input from ascending neurons from the VNC conveying somatosensory information from the legs (Tsubouchi *et al.*, 2017). Interestingly, calcium imaging revealed a spatial map for the AVLP and wedge (WED) with neurons responding primarily to movement of fore-, mid- or hindlegs (Tsubouchi *et al.*, 2017). The role in walk of the region strongly inhibited we termed AVLPshell was not studied yet, to our knowledge. The functional component maps matched to anatomical templates should thus be helpful in identifying neurons within these regions and their respective functions during walk.

Advantages and limitation of the method

Our study has several advantages and limitations. First, the lightfield speed –significantly higher temporal resolution as compared to sequential scanning methods– allowed us to record whole brain activity at the same time as fast behavioral patterns. However, GCaMP dynamics and limitations in signal to noise ratio rarely permitted us to resolve single action potentials, so we might be missing important computational aspects. Second, functional units might not be neurons in the fly, but rather micronetworks due to the strong non-synaptic coupling and the many non-spiking neurons. The spatial resolution of lightfield imaging is inferior to confocal or volumetric multiphoton imaging. Although these methods do not allow resolving single neurites with pan-neuronally expressed sensors, lightfield could make it even more difficult to detect whether neurites could act as independent functional units. On the other hand, capturing the whole volume simultaneously makes it easier to unmix signals as we showed with our PCA/ICA approach which partially compensates for the lower spatial resolution. Third, our data is based on observations without genetic or functional manipulation of neurons or circuits. Excitation and inhibition of single neurons are being carried out very frequently in *Drosophila* thanks to its unique genetic tools. We believe that our data complements previous and future functional studies as imaging or manipulation of individual neurons provides only limited insights into the role and effect of a neuron in the complex dynamic neural networks in which they are embedded. Indeed, the response of one neuron relative to the rest of the network is likely to be important (even simplest model neurons integrate activity from several input neurons in a timely fashion). In the future, a combination of single neuron manipulation and wholebrain imaging will likely lead to unexpected insights into the relationship of a neuron and a specific behavior. Fourth, we have observed subtler differences between flies that are obvious from individual experiments but difficult to capture quantitatively across a population of animals. These subtle differences might be resolvable by greatly increasing the number of experiments. Given the technical difficulty of the preparation method, reaching high animal numbers will be extremely challenging but perhaps possible in the future. Finally, together with the now available wholebrain EM connectome, our data provides a timely resource for the community of fly neuroscientists interested in linking neuronal activity to behavior.

Conclusions

We provide an overview of brain activity during simple behaviors in *Drosophila*. As for other animals, *Drosophila* brain activity is globally correlated with locomotion leading to global change in brain state. However, our results challenge the assumption that most of the activity is related

to decision-making, top-down motor control, or prediction error detection from sensory feedback and instead suggest that walk itself and somatosensory bottom-up stimuli are largely responsible. By using a combination of pan-neuronal and specific neuron line imaging, we shed light on the nature of neurons and their location in the brain that respond so strongly to behavior. Altogether, our data provide a novel resource for further generating new hypotheses regarding the brain-behavior-loop and for dissecting the neural circuits underpinning it.

Materials and Methods

Fly rearing

We used one to four days old female flies raised at 25 °C. Most flies were starved 24 or 48h with a water only environment, and we clipped the wings at least one day in advance. Experiments were performed in the evening peak of circadian activity (ZT0 or ZT11) and we heated the room to ~28 °C during the experiment.

Fly preparation for imaging

We prepared the flies as described in details in (Woller *et al.*, 2021). Briefly, we fixed a fly to a home designed 3D printed holder, so as to allow access to the whole posterior side of the head while the legs were free to move. We added saline (103 mM NaCl, 3 mM KCl, 5 mM TES, 8 mM trehalose 2 H2O, 10 mM glucose, 26 mM NaHCO3, 1 mM NaH2PO4, 2.5 mM CaCl2·2 H2O, 4 mM MgCl2·6 H2O) and dissected the cuticle, muscles and air sacks at the back of the head.

Walk substrates

For studying spontaneous walk, we used two types of small balls. One was an air-supported ball as previously described (Sayin *et al.*, 2019; Seelig *et al.*, 2010). As we wanted to make sure the walk was initiated by the fly rather than erratic movement of the ball we also used small styrofoam balls that were held by the fly. In both preparations, flies walked spontaneously and the brain activity elicted by spontaneous walk was not significantly different between the preparations. Therefore, these data were combined in all analysis.

As treadmill for studying forced walk, we used small motors (DC 6V gear motor with long M3 x 55mm lead screw thread output shaft speed reducer Walfront Store, www.amazon.de), covered with self-curing rubber (from Sugru) to provide a smoother surface.

In vivo lightfield imaging

Fast volumetric imaging was performed using lightfield imaging – in which a microlens array separates rays- from different angles to give information on depth -- was carried out as previously described (Aimon *et al.*, 2019). Some of the datasets were previously published in Aimon et al. (Aimon *et al.*, 2019) and source data (http://dx.doi.org/10.6080/K01J97ZN), with a microscope equipped with a 20x NA1.0 objective. Most data was obtained with a lightfield

microscope constituted of a Thorlabs Cerna system with a Leica HC FLUOTAR L 25x/0.95 objective and an MLA-S125-f12 microlens array (Viavi). The microlens array was placed on the image plane, while the camera imaged the microlens array through 50 mm f/1.4 NIKKOR-S Nikon relay lenses. The light field images were recorded with a scientific CMOS camera (Hamamatsu ORCA-Flash 4.0). The volumes were reconstructed offline, using a python program developed by (Broxton et al., 2013) and available on github: https://github.com/sophie63/FlyLFM.

Behavior recording and scoring

We imaged the fly and substrate movements using infra red illumination and two small cameras FFMV-03M2M from Point Grey triggered by the fluorescence recording camera to ensure time alignment between fluorescence and behavior.

Walking, flailing and grooming were obtained by measuring the optic flow from the videos of the ball or by analyzing the movement of the fly's legs using the "optic flow" plugin in FIJI. The results were checked by hand and binarized (e.g. walking vs. not walking). For turning, the sum of left or right optic flows was not binarized. The behavioral time series were then convolved with the single spike response of the GCaMP version used for the experiment, and subjected to the same deltaF/F procedure as the fluorescence time series (see below).

Pre-processing

Reconstructed volumetric fluorescence data was pre-processed by first correcting for movement using 3Dvolreg from AFNI (Cox and Jesmanowicz, 1999). In Matlab, we then calculated the deltaF/F for each voxel by subtracting and dividing by the signal averaged for 4000 time points. We finally decreased noise with a Kalman filter (from https://www.mathworks.com/matlabcentral/fileexchange/26334-kalman-filter-for-noisy-movies) with a gain of 0.5.

We generated summary movies by maximum projecting the $\Delta F/F$ volumes and combining these to the behavior.

Alignment to template

We aligned the functional data to anatomical templates using landmarks registration with ImageJ (as described in http://imagej.net/Name_Landmarks_and_Register).

PCA/ICA

To obtain functional maps of the fly brain, we performed PCA and ICA as described previously (Aimon *et al.*, 2019; Beckmann et al., 2020). Briefly, SVD was used a first time to find the level of noise and normalize voxels by their noise variance. SVD was performed a second time on this normalized data resulting in maps and time series for principal components. The principal component maps were unmixed using ICA to obtain localized regions. The same matrix was used to unmix the time series.

The functional regions were aligned with anatomical templates as described above. This allowed finding the anatomically defined regions covered by the functional regions (see Table 2), and find candidate neurons (using Flycircuit (http://www.flycircuit.tw/) or Virtual Fly Brain https://v2.virtualflybrain.org) data bases).

Statistics

Statistics were performed in python with code freely available on https://github.com/sophie63/Aimon2022. To compare fluorescence time series (normalized by the absolute maximum value per fly) and behavioral time series, we used a simple regression model: TSfluo ~ BehaviorRegressor, solved with the ordinary least square fit function of the python statsmodels package. For each time series (either regional averaged intensity of the PCA/ICA component), this provided a fraction of variance explained by the behavior (R^2), and the sign and strength of the correlation (coefficient). We compared these values with pair-wise tests using Mann-Withney non-parametric tests with a Bonferroni multiple comparison correction.

We used a linear model to evaluate the effect of variables of interest (behavior, brain region, neural type) while explaining away confounds (GCaMP version, exact pan neuronal GAL4): R2 ~ Behavior+RegionNames+GAL4+UAS. We then plotted the coeffcients + intercept, and 95% interval of coefficient + 95% interval of the intercept to compare the effect of the variables to zero.

Author contributions

SA developed the preparation, made the initial observation, and generated most data sets. KC generated additional datasets. SA analyzed the data with the help of KC. JG and IGK oversaw the study. SA and IGK wrote the paper with help and input by all other authors.

Acknowledgments

We are very grateful to Marta Costa and Kei Ito for sharing data, images, and knowledge during the course of this study. We also thank Francisco Rodriguez-Jimenez, Paul Bandow, Subhadarshini Parhi and Kunhi Purayil Siju for help with data analysis.

References

Ache, J.M., Namiki, S., Lee, A., Branson, K., and Card, G.M. (2019). State-dependent decoupling of sensory and motor circuits underlies behavioral flexibility in Drosophila. Nat Neurosci *22*, 1132-1139. 10.1038/s41593-019-0413-4.

Agrawal, S., Dickinson, E.S., Sustar, A., Gurung, P., Shepherd, D., Truman, J.W., and Tuthill, J.C. (2020). Central processing of leg proprioception in Drosophila. Elife *9*. 10.7554/eLife.60299.

Aimon, S., Katsuki, T., Jia, T., Grosenick, L., Broxton, M., Deisseroth, K., Sejnowski, T.J., and Greenspan, R.J. (2019). Fast near-whole-brain imaging in adult Drosophila during responses to stimuli and behavior. PLoS Biol *17*, e2006732. 10.1371/journal.pbio.2006732.

Allen, A.M., Neville, M.C., Birtles, S., Croset, V., Treiber, C.D., Waddell, S., and Goodwin, S.F. (2020). A single-cell transcriptomic atlas of the adult Drosophila ventral nerve cord. Elife *9*. 10.7554/eLife.54074.

Aonuma, H. (2020). Serotonergic control in initiating defensive responses to unexpected tactile stimuli in the trap-jaw ant Odontomachus kuroiwae. J Exp Biol *223*. 10.1242/jeb.228874.

Azanchi, R., Kaun, K.R., and Heberlein, U. (2013). Competing dopamine neurons drive oviposition choice for ethanol in Drosophila. Proc Natl Acad Sci U S A *110*, 21153-21158. 10.1073/pnas.1320208110.

Beckmann, K.M., Wang-Leandro, A., Dennler, M., Carrera, I., Richter, H., Bektas, R.N., Steiner, A., and Haller, S. (2020). Resting state networks of the canine brain under sevoflurane anaesthesia. PLoS One *15*, e0231955. 10.1371/journal.pone.0231955.

Benjamin, P.R., Staras, K., and Kemenes, G. (2010). What roles do tonic inhibition and disinhibition play in the control of motor programs? Front Behav Neurosci *4*, 30. 10.3389/fnbeh.2010.00030.

Berman, G.J., Bialek, W., and Shaevitz, J.W. (2016). Predictability and hierarchy in Drosophila behavior. Proc Natl Acad Sci U S A *113*, 11943-11948. 10.1073/pnas.1607601113.

Berry, J.A., Cervantes-Sandoval, I., Chakraborty, M., and Davis, R.L. (2015). Sleep Facilitates Memory by Blocking Dopamine Neuron-Mediated Forgetting. Cell *161*, 1656-1667. 10.1016/j.cell.2015.05.027.

Bidaye, S.S., Laturney, M., Chang, A.K., Liu, Y., Bockemuhl, T., Buschges, A., and Scott, K. (2020). Two Brain Pathways Initiate Distinct Forward Walking Programs in Drosophila. Neuron *108*, 469-485 e468. 10.1016/j.neuron.2020.07.032.

Bidaye, S.S., Machacek, C., Wu, Y., and Dickson, B.J. (2014). Neuronal control of Drosophila walking direction. Science *344*, 97-101. 10.1126/science.1249964.

Borst, A., Haag, J., and Mauss, A.S. (2020). How fly neurons compute the direction of visual motion. J Comp Physiol A Neuroethol Sens Neural Behav Physiol *206*, 109-124. 10.1007/s00359-019-01375-9.

Brembs, B., Christiansen, F., Pfluger, H.J., and Duch, C. (2007). Flight initiation and maintenance deficits in flies with genetically altered biogenic amine levels. J Neurosci *27*, 11122-11131. 10.1523/JNEUROSCI.2704-07.2007.

Broxton, M., Grosenick, L., Yang, S., Cohen, N., Andalman, A., Deisseroth, K., and Levoy, M. (2013). Wave optics theory and 3-D deconvolution for the light field microscope. Optics express *21*, 25418-25439. 10.1364/OE.21.025418.

Busch, S., Selcho, M., Ito, K., and Tanimoto, H. (2009). A map of octopaminergic neurons in the Drosophila brain. J Comp Neurol *513*, 643-667. 10.1002/cne.21966.

Busse, L., Cardin, J.A., Chiappe, M.E., Halassa, M.M., McGinley, M.J., Yamashita, T., and Saleem, A.B. (2017). Sensation during Active Behaviors. J Neurosci *37*, 10826-10834. 10.1523/JNEUROSCI.1828-17.2017.

Calhoun, A.J., Pillow, J.W., and Murthy, M. (2019). Author Correction: Unsupervised identification of the internal states that shape natural behavior. Nat Neurosci. 10.1038/s41593-019-0571-4.

Chapman, P.D., Burkland, R., Bradley, S.P., Houot, B., Bullman, V., Dacks, A.M., and Daly, K.C. (2018). Flight motor networks modulate primary olfactory processing in the moth Manduca sexta. Proc Natl Acad Sci U S A *115*, 5588-5593. 10.1073/pnas.1722379115.

Chen, C.L., Hermans, L., Viswanathan, M.C., Fortun, D., Aymanns, F., Unser, M., Cammarato, A., Dickinson, M.H., and Ramdya, P. (2018). Imaging neural activity in the ventral nerve cord of behaving adult Drosophila. Nat Commun *9*, 4390. 10.1038/s41467-018-06857-z.

Chiang, A.S., Lin, C.Y., Chuang, C.C., Chang, H.M., Hsieh, C.H., Yeh, C.W., Shih, C.T., Wu, J.J., Wang, G.T., Chen, Y.C., et al. (2011). Three-dimensional reconstruction of brain-wide wiring networks in Drosophila at single-cell resolution. Curr Biol *21*, 1-11. 10.1016/j.cub.2010.11.056.

Chiappe, M.E., Seelig, J.D., Reiser, M.B., and Jayaraman, V. (2010). Walking modulates speed sensitivity in Drosophila motion vision. Curr Biol *20*, 1470-1475. 10.1016/j.cub.2010.06.072.

Coates, K.E., Calle-Schuler, S.A., Helmick, L.M., Knotts, V.L., Martik, B.N., Salman, F., Warner, L.T., Valla, S.V., Bock, D.D., and Dacks, A.M. (2020). The Wiring Logic of an Identified Serotonergic Neuron That Spans Sensory Networks. J Neurosci *40*, 6309-6327. 10.1523/JNEUROSCI.0552-20.2020.

Cohn, R., Morantte, I., and Ruta, V. (2015). Coordinated and Compartmentalized Neuromodulation Shapes Sensory Processing in Drosophila. Cell *163*, 1742-1755. 10.1016/j.cell.2015.11.019.

Collins, L., Boddington, L., Steffan, P.J., and McCormick, D. (2021). Vagus nerve stimulation induces widespread cortical and behavioral activation. Curr Biol *31*, 2088-2098 e2083. 10.1016/j.cub.2021.02.049.

Cox, R.W., and Jesmanowicz, A. (1999). Real-time 3D image registration for functional MRI. Magn Reson Med *42*, 1014-1018. 10.1002/(sici)1522-2594(199912)42:6<1014::aid-mrm4>3.0.co;2-f.

Creamer, M.S., Mano, O., and Clark, D.A. (2018). Visual Control of Walking Speed in Drosophila. Neuron *100*, 1460-1473 e1466. 10.1016/j.neuron.2018.10.028.

Cruz, T.L., Perez, S.M., and Chiappe, M.E. (2021). Fast tuning of posture control by visual feedback underlies gaze stabilization in walking Drosophila. Curr Biol. 10.1016/j.cub.2021.08.041.

DeAngelis, B.D., Zavatone-Veth, J.A., and Clark, D.A. (2019). The manifold structure of limb coordination in walking Drosophila. Elife *8*. 10.7554/eLife.46409.

Emanuel, S., Kaiser, M., Pflueger, H.J., and Libersat, F. (2020). On the Role of the Head Ganglia in Posture and Walking in Insects. Front Physiol *11*, 135. 10.3389/fphys.2020.00135.

Fenk, L.M., Kim, A.J., and Maimon, G. (2021). Suppression of motion vision during course-changing, but not course-stabilizing, navigational turns. Curr Biol. 10.1016/j.cub.2021.09.068.
Flaive, A., Fougere, M., van der Zouwen, C.I., and Ryczko, D. (2020). Serotonergic Modulation of Locomotor Activity From Basal Vertebrates to Mammals. Front Neural Circuits *14*, 590299. 10.3389/fncir.2020.590299.
Friston, K. (2005). A theory of cortical responses. Philos Trans R Soc Lond B Biol Sci *360*, 815-836. 10.1098/rstb.2005.1622.
Fu, Y., Tucciarone, J.M., Espinosa, J.S., Sheng, N., Darcy, D.P., Nicoll, R.A., Huang, Z.J., and Stryker, M.P. (2014). A cortical circuit for gain control by behavioral state. Cell *156*, 1139-1152. 10.1016/j.cell.2014.01.050.
Fujiwara, T., Cruz, T.L., Bohnslav, J.P., and Chiappe, M.E. (2017). A faithful internal representation of walking movements in the Drosophila visual system. Nat Neurosci *20*, 72-81. 10.1038/nn.4435.
Geurten, B.R., Jahde, P., Corthals, K., and Gopfert, M.C. (2014). Saccadic body turns in walking Drosophila. Front Behav Neurosci *8*, 365. 10.3389/fnbeh.2014.00365.
Haesemeyer, M., Robson, D.N., Li, J.M., Schier, A.F., and Engert, F. (2018). A Brain-wide Circuit Model of Heat-Evoked Swimming Behavior in Larval Zebrafish. Neuron *98*, 817-831 e816. 10.1016/j.neuron.2018.04.013.
Hampel, S., Franconville, R., Simpson, J.H., and Seeds, A.M. (2015). A neural command circuit for grooming movement control. Elife *4*, e08758. 10.7554/eLife.08758.
Helfrich-Förster, C. (2018). Sleep in Insects. Annu Rev Entomol *63*, 69-86. 10.1146/annurev-ento-020117-043201.
Henschke, J.U., Price, A.T., and Pakan, J.M.P. (2021). Enhanced modulation of cell-type specific neuronal responses in mouse dorsal auditory field during locomotion. Cell Calcium *96*, 102390. 10.1016/j.ceca.2021.102390.
Hsu, C.T., and Bhandawat, V. (2016). Organization of descending neurons in Drosophila melanogaster. Sci Rep *6*, 20259. 10.1038/srep20259.
Ito, K., Shinomiya, K., Ito, M., Armstrong, J.D., Boyan, G., Hartenstein, V., Harzsch, S., Heisenberg, M., Homberg, U., Jenett, A., et al. (2014). A systematic nomenclature for the insect brain. Neuron *81*, 755-765. 10.1016/j.neuron.2013.12.017.
Kaplan, H.S., and Zimmer, M. (2020). Brain-wide representations of ongoing behavior: a universal principle? Curr Opin Neurobiol *64*, 60-69. 10.1016/j.conb.2020.02.008.
Kato, S., Kaplan, H.S., Schrodel, T., Skora, S., Lindsay, T.H., Yemini, E., Lockery, S., and Zimmer, M. (2015). Global brain dynamics embed the motor command sequence of Caenorhabditis elegans. Cell *163*, 656-669. 10.1016/j.cell.2015.09.034.
Katsov, A.Y., Freifeld, L., Horowitz, M., Kuehn, S., and Clandinin, T.R. (2017). Dynamic structure of locomotor behavior in walking fruit flies. Elife *6*. 10.7554/eLife.26410.
Keller, G.B., and Mrsic-Flogel, T.D. (2018). Predictive Processing: A Canonical Cortical Computation. Neuron *100*, 424-435. 10.1016/j.neuron.2018.10.003.
Kien, J. (1990a). Neuronal activity during spontaneous walking--I. Starting and stopping. Comparative biochemistry and physiology. A, Comparative physiology *95*, 607-621. 10.1016/0300-9629(90)90747-g.
Kien, J. (1990b). Neuronal activity during spontaneous walking--II. Correlation with stepping. Comparative biochemistry and physiology. A, Comparative physiology *95*, 623-638. 10.1016/0300-9629(90)90748-h.
Lee, Y.J., Yang, C.P., Miyares, R.L., Huang, Y.F., He, Y., Ren, Q., Chen, H.M., Kawase, T., Ito, M., Otsuna, H., et al. (2020). Conservation and divergence of related neuronal lineages in the Drosophila central brain. Elife *9*. 10.7554/eLife.53518.
Li, Y., Tiedemann, L., von Frieling, J., Nolte, S., El-Kholy, S., Stephano, F., Gelhaus, C., Bruchhaus, I., Fink, C., and Roeder, T. (2017). The Role of Monoaminergic Neurotransmission

for Metabolic Control in the Fruit Fly Drosophila Melanogaster. Front Syst Neurosci *11*, 60. 10.3389/fnsys.2017.00060.
Liu, C., Placais, P.Y., Yamagata, N., Pfeiffer, B.D., Aso, Y., Friedrich, A.B., Siwanowicz, I., Rubin, G.M., Preat, T., and Tanimoto, H. (2012). A subset of dopamine neurons signals reward for odour memory in Drosophila. Nature *488*, 512-516. 10.1038/nature11304.
Lu, J., Behbahani, A.H., Hamburg, L., Westeinde, E.A., Dawson, P.M., Lyu, C., Maimon, G., Dickinson, M.H., Druckmann, S., and Wilson, R.I. (2021). Transforming representations of movement from body- to world-centric space. Nature. 10.1038/s41586-021-04191-x.
Mace, E., Montaldo, G., Trenholm, S., Cowan, C., Brignall, A., Urban, A., and Roska, B. (2018). Whole-Brain Functional Ultrasound Imaging Reveals Brain Modules for Visuomotor Integration. Neuron *100*, 1241-1251 e1247. 10.1016/j.neuron.2018.11.031.
Maimon, G., Straw, A.D., and Dickinson, M.H. (2010). Active flight increases the gain of visual motion processing in Drosophila. Nat Neurosci *13*, 393-399. 10.1038/nn.2492.
Mamiya, A., Gurung, P., and Tuthill, J.C. (2018). Neural Coding of Leg Proprioception in Drosophila. Neuron *100*, 636-650 e636. 10.1016/j.neuron.2018.09.009.
Mao, Z., and Davis, R.L. (2009). Eight different types of dopaminergic neurons innervate the Drosophila mushroom body neuropil: anatomical and physiological heterogeneity. Front Neural Circuits *3*, 5. 10.3389/neuro.04.005.2009.
Mendes, C.S., Rajendren, S.V., Bartos, I., Marka, S., and Mann, R.S. (2014). Kinematic responses to changes in walking orientation and gravitational load in Drosophila melanogaster. PLoS One *9*, e109204. 10.1371/journal.pone.0109204.
Mu, Y., Bennett, D.V., Rubinov, M., Narayan, S., Yang, C.T., Tanimoto, M., Mensh, B.D., Looger, L.L., and Ahrens, M.B. (2019). Glia Accumulate Evidence that Actions Are Futile and Suppress Unsuccessful Behavior. Cell *178*, 27-43 e19. 10.1016/j.cell.2019.05.050.
Mueller, J.M., Ravbar, P., Simpson, J.H., and Carlson, J.M. (2019). Drosophila melanogaster grooming possesses syntax with distinct rules at different temporal scales. PLoS Comput Biol *15*, e1007105. 10.1371/journal.pcbi.1007105.
Musall, S., Kaufman, M.T., Juavinett, A.L., Gluf, S., and Churchland, A.K. (2019). Single-trial neural dynamics are dominated by richly varied movements. Nat Neurosci *22*, 1677-1686. 10.1038/s41593-019-0502-4.
Ngai, M., Shoue, D.A., Loh, Z., and McDowell, M.A. (2019). The pharmacological and functional characterization of the serotonergic system in Anopheles gambiae and Aedes aegypti: influences on flight and blood-feeding behavior. Sci Rep *9*, 4421. 10.1038/s41598-019-38806-1.
Parker, P.R.L., Brown, M.A., Smear, M.C., and Niell, C.M. (2020). Movement-Related Signals in Sensory Areas: Roles in Natural Behavior. Trends Neurosci *43*, 581-595. 10.1016/j.tins.2020.05.005.
Reimer, J., McGinley, M.J., Liu, Y., Rodenkirch, C., Wang, Q., McCormick, D.A., and Tolias, A.S. (2016). Pupil fluctuations track rapid changes in adrenergic and cholinergic activity in cortex. Nat Commun *7*, 13289. 10.1038/ncomms13289.
Sayin, S., De Backer, J.F., Siju, K.P., Wosniack, M.E., Lewis, L.P., Frisch, L.M., Gansen, B., Schlegel, P., Edmondson-Stait, A., Sharifi, N., et al. (2019). A Neural Circuit Arbitrates between Persistence and Withdrawal in Hungry Drosophila. Neuron *104*, 544-558 e546. 10.1016/j.neuron.2019.07.028.
Scheffer, L.K., Xu, C.S., Januszewski, M., Lu, Z., Takemura, S.Y., Hayworth, K.J., Huang, G.B., Shinomiya, K., Maitlin-Shepard, J., Berg, S., et al. (2020). A connectome and analysis of the adult Drosophila central brain. Elife *9*. 10.7554/eLife.57443.
Schilling, M., and Cruse, H. (2020). Decentralized control of insect walking: A simple neural network explains a wide range of behavioral and neurophysiological results. PLoS Comput Biol *16*, e1007804. 10.1371/journal.pcbi.1007804.

Schoofs, A., Huckesfeld, S., and Pankratz, M.J. (2018). Serotonergic network in the subesophageal zone modulates the motor pattern for food intake in Drosophila. J Insect Physiol *106*, 36-46. 10.1016/j.jinsphys.2017.07.007.

Schoofs, A., Huckesfeld, S., Surendran, S., and Pankratz, M.J. (2014). Serotonergic pathways in the Drosophila larval enteric nervous system. J Insect Physiol *69*, 118-125. 10.1016/j.jinsphys.2014.05.022.

Seelig, J.D., Chiappe, M.E., Lott, G.K., Dutta, A., Osborne, J.E., Reiser, M.B., and Jayaraman, V. (2010). Two-photon calcium imaging from head-fixed Drosophila during optomotor walking behavior. Nat Methods *7*, 535-540. 10.1038/nmeth.1468.

Sen, R., Wang, K., and Dickson, B.J. (2019). TwoLumps Ascending Neurons Mediate Touch-Evoked Reversal of Walking Direction in Drosophila. Curr Biol *29*, 4337-4344 e4335. 10.1016/j.cub.2019.11.004.

Siju, K.P., Stih, V., Aimon, S., Gjorgjieva, J., Portugues, R., and Grunwald Kadow, I.C. (2020). Valence and State-Dependent Population Coding in Dopaminergic Neurons in the Fly Mushroom Body. Curr Biol *30*, 2104-2115 e2104. 10.1016/j.cub.2020.04.037.

Sims, D.W., Humphries, N.E., Hu, N., Medan, V., and Berni, J. (2019). Optimal searching behaviour generated intrinsically by the central pattern generator for locomotion. Elife *8*. 10.7554/eLife.50316.

Stringer, C., Pachitariu, M., Steinmetz, N., Reddy, C.B., Carandini, M., and Harris, K.D. (2019). Spontaneous behaviors drive multidimensional, brainwide activity. Science *364*, 255. 10.1126/science.aav7893.

Suver, M.P., Huda, A., Iwasaki, N., Safarik, S., and Dickinson, M.H. (2016). An Array of Descending Visual Interneurons Encoding Self-Motion in Drosophila. J Neurosci *36*, 11768-11780. 10.1523/JNEUROSCI.2277-16.2016.

Tantirigama, M.L.S., Zolnik, T., Judkewitz, B., Larkum, M.E., and Sachdev, R.N.S. (2020). Perspective on the Multiple Pathways to Changing Brain States. Front Syst Neurosci *14*, 23. 10.3389/fnsys.2020.00023.

Tao, L., Ozarkar, S., Beck, J.M., and Bhandawat, V. (2019). Statistical structure of locomotion and its modulation by odors. Elife *8*. 10.7554/eLife.41235.

Tsai, K.T., and Chou, Y.H. (2019). Random Walk Revisited: Quantification and Comparative Analysis of Drosophila Walking Trajectories. iScience *19*, 1145-1159. 10.1016/j.isci.2019.08.054.

Tsubouchi, A., Yano, T., Yokoyama, T.K., Murtin, C., Otsuna, H., and Ito, K. (2017). Topological and modality-specific representation of somatosensory information in the fly brain. Science *358*, 615-623. 10.1126/science.aan4428.

Vicente, A.M., Martins, G.J., and Costa, R.M. (2020). Cortico-basal ganglia circuits underlying dysfunctional control of motor behaviors in neuropsychiatric disorders. Curr Opin Genet Dev *65*, 151-159. 10.1016/j.gde.2020.05.042.

Vitrac, C., and Benoit-Marand, M. (2017). Monoaminergic Modulation of Motor Cortex Function. Front Neural Circuits *11*, 72. 10.3389/fncir.2017.00072.

von Philipsborn, A.C., Liu, T., Yu, J.Y., Masser, C., Bidaye, S.S., and Dickson, B.J. (2011). Neuronal control of Drosophila courtship song. Neuron *69*, 509-522. 10.1016/j.neuron.2011.01.011.

Woller, A., Bandow, P., Aimon, S., and Grunwald Kadow, I.C. (2021). Preparing Adult Drosophila melanogaster for Whole Brain Imaging during Behavior and Stimuli Responses. J Vis Exp. 10.3791/61876.

Wolpert, D.M., Diedrichsen, J., and Flanagan, J.R. (2011). Principles of sensorimotor learning. Nat Rev Neurosci *12*, 739-751. 10.1038/nrn3112.

Zacarias, R., Namiki, S., Card, G.M., Vasconcelos, M.L., and Moita, M.A. (2018). Speed dependent descending control of freezing behavior in Drosophila melanogaster. Nat Commun *9*, 3697. 10.1038/s41467-018-05875-1.

Zolin, A., Cohn, R., Pang, R., Siliciano, A.F., Fairhall, A.L., and Ruta, V. (2021). Context-dependent representations of movement in Drosophila dopaminergic reinforcement pathways. Nat Neurosci *24*, 1555-1566. 10.1038/s41593-021-00929-y.